ELSEVIER

Biochimica et Biophysica Acta 1281 (1996) 139–149

BBA Biochimica et Biophysica Acta

Fate of cationic liposomes and their complex with oligonucleotide in vivo

David C. Litzinger [a,*], Jeffrey M. Brown [a], Iwona Wala [a], Stephen A. Kaufman [b], Gwyneth Y. Van [b], Catherine L. Farrell [c], David Collins [a]

[a] *Department of Pharmacology, Amgen, Inc., Thousand Oaks, CA 91320, USA*
[b] *Department of Anatomical Pathology, Amgen, Inc., Thousand Oaks, CA 91320, USA*
[c] *Department of Experimental Pathology, Amgen, Inc., Thousand Oaks, CA 91320, USA*

Received 14 August 1995; accepted 20 October 1995

Abstract

The present studies describe the biodistribution of cationic liposomes and cationic liposome/oligonucleotide complex following intravenous injection into mice via the tail vein. ^{111}In-diethylenetriaminepentaacetic acid stearylamide (^{111}In-DTPA-SA) was used as a lipid-phase radiolabel. Inclusion of up to 5 mol% DTPA-SA in liposomes composed of 3β-(*N*-(*N'*,*N'*-dimethylaminoethane)carbamoyl)cholesterol (DC-Chol) and dioleoylphosphatidylethanolamine (DOPE) did not influence liposome formation or size, nor the binding/uptake or fusion of the cationic liposomes with CHO cells in vitro. Moreover, nuclear delivery of oligonucleotide to CHO cells was unaffected by the probe. The biodistribution of liposomes with increasing concentration of DC-Chol (1:4–4:1, DC-Chol/DOPE, mol/mol) at 24 h post-injection revealed no dependence on lipid composition. Uptake was primarily by liver, and accumulation in spleen and skin was also observed. Comparatively little accumulation occurred in lung. Clearance of injected liposomes by liver was very rapid (~ 84.5% of the injected dose by 7.5 h post-injection). Liposome uptake by liver and spleen were equally efficient in the dose range of 3.33 to 33.33 mg/kg body weight, yet possible saturation of liver uptake at a dose of 66.80 mg/kg may have allowed for increased spleen accumulation. Preincubation of cationic liposomes with phosphorothioate oligonucleotide induced a dramatic yet transient accumulation of the lipid in lung which gradually redistributed to liver. Similar results were observed when monitoring iodinated oligonucleotide in the complex. Immuno-histochemical studies revealed large aggregates of oligonucleotide within pulmonary capillaries at 15 min post-injection, suggesting the early accumulation in lung was due to embolism. Immuno-histochemical studies further revealed labeled oligonucleotide to be localized primarily to Kupffer cells at 24 h post-injection. Immuno-electron microscopy revealed localization of oligonucleotide primarily to the lumen of pulmonary capillaries at 15 min post-injection, and to phagocytic vacuoles of Kupffer cells at 24 h post-injection. By these methods, nuclear delivery of oligonucleotide in vivo was not observed. Increasing concentration of mouse serum inhibited cellular binding/uptake of cationic liposomes in vitro, without or with complexed oligonucleotide. We therefore postulate that interaction with plasma components, including opsonin(s), inhibits cellular uptake of the injected liposomes as well as the liposome/oligonucleotide complex, and mediates rapid uptake by Kupffer cells of the liver. These results are relevant to the design of cationic liposomes for efficient delivery of nucleic acid in vivo.

Keywords: Liposome; Cationic liposome; Oligonucleotide; Biodistribution; Antisense therapy

1. Introduction

Antisense oligonucleotides are in development by several groups with the prospect of arresting the expression of specifically targeted genes. The mechanism for such inhibition may primarily be via RNase hydrolysis of the RNA strand of the target mRNA-oligonucleotide duplex. However, other mechanisms including transcription inhibition following the formation of a DNA-oligonucleotide triplex,

Abbreviations: BrdU, 5-bromodeoxyuridine; CHO, Chinese hamster ovary; D-PBS, Dulbecco's phosphate-buffered saline; DC-Chol, 3β-(*N*-(*N'*,*N'*-dimethylaminoethane)carbamoyl)cholesterol; DOPE, dioleoylphosphatidylethanolamine; DTPA-SA, diethylenetriaminepentaacetic acid stearylamide; GAR, goat anti-rat; ^{3}H-CE, hexadecyl [^{3}H]cholestanyl ether; PS, phosphatidylserine; Pyr-PC, 3-palmitoyl-2-(1-pyrenedecanoyl)phosphatidylcholine; SA, stearylamine.

* Corresponding author. Fax: +1 (805) 4988674.

SSDI 0005-2736(95)00268-5

and the inhibition of mRNA transport to the cytoplasm have been proposed [1]. Efforts to improve the potency of antisense oligonucleotides include the synthesis of nuclease-resistant oligonucleotides. Introduction of phosphorothioate linkages has been shown to confer nuclease resistance [2]. Furthermore, circulating phosphorothioated oligonucleotides in vivo appear to remain intact for over 24 h [3].

The inability of oligonucleotides to efficiently traverse through cellular membranes poses a major obstacle for activity. While nuclear delivery of oligonucleotides can be achieved in vitro by microinjection, simple incubation of the fluorescently-labeled oligonucleotides with cells results in accumulation in cytoplasmic granules and no fluorescence in the nucleus [4].

However, cationic liposomes have been shown to markedly increase the association of oligonucleotide with cells in vitro [5]. Furthermore, oligonucleotide complexed with cationic liposomes and subsequently incubated with cells localized within the nucleus, as well as to discrete structures in the cytoplasm [4,5]. Moreover, cationic liposomes have been shown to greatly enhance the potency of antisense oligonucleotides in vitro [5,6].

Liposomes composed of the cationic lipid 3β-(*N*-(*N'*,*N'*-dimethylaminoethane)carbamoyl)cholesterol (DC-Chol) together with dioleoylphosphatidylethanolamine (DOPE) have demonstrated efficient transfection of cells in vitro with plasmid DNA [7]. DC-Chol is stable and has low toxicity [7], presumably due to biodegradability. Transfection of malignant tumors in vivo by direct injection of DC-Chol/DOPE liposome/DNA complex into exposed tumor has been demonstrated [8]. DC-Chol/DOPE liposomes also mediate nuclear delivery of oligonucleotide to cells in vitro (D. Collins, unpublished data).

To evaluate the potential of cationic liposomes as a reagent for antisense oligonucleotide therapy, we examined the biodistribution of cationic liposomes and cationic liposomes complexed with oligonucleotide in vivo following intravenous injection. Our studies demonstrate that cationic liposomes are rapidly cleared by liver. Complexation of the liposomes with oligonucleotide induced a dramatic yet transient accumulation in lung. Both the lipid and oligonucleotide were cleared from the lung and subsequently accumulated in liver. Immuno-histochemistry and immuno-electron microscopy results suggest the lung accumulation of the complex is primarily due to embolism, and the subsequent liver accumulation is localized primarily to the Kupffer cells. By our methods, nuclear delivery of oligonucleotide in vivo was not observed. Furthermore, our studies show that binding/uptake of cationic liposomes both alone, or complexed with oligonucleotide, by cells in vitro is inhibited by serum. We propose that interaction with plasma components, including opsonin(s), must be reduced in order for cationic liposomes to be used for efficient nuclear delivery of oligonucleotide in vivo.

2. Materials and methods

2.1. Materials

DOPE was purchased from Avanti Polar Lipids (Alabaster, AL) and Chol was obtained from Sigma (St. Louis, MO). $^{111}InCl_3$ (carrier-free) and ^{125}I were from New England Nuclear (Boston, MA). DTPA-SA was synthesized as described [9], and ^{111}In-labeled DTPA-SA (^{111}In-DTPA-SA) was prepared as described [10]. DC-Chol was synthesized as described [7]. CHO D$^-$ cells were obtained from Dr. G. Trail (Amgen) and were grown in RPMI 1640, containing 10% FBS and 1% penicillin/streptomycin/glutamine. Pyr-PC was purchased from Molecular Probes (Eugene, OR). LS2-1, a fully phosphorothioated 18mer oligonucleotide, and F15-27, a BrdU-labeled analog of LS2-1, were synthesized at Amgen Boulder. FITC-labeled phosphorothioated 18mer oligonucleotide was also synthesized at Amgen Boulder. D-PBS was obtained from Gibco, BRL (Gaithersburg, MD).

2.2. Liposome and liposome/oligonucleotide complex preparation

Lipid mixtures containing trace amounts of ^{111}In-DTPA-SA or hexadecyl [^{3}H]cholestanyl ether (^{3}H-CE) were dried from organic solvent with N_2 gas and vacuum desiccated for 0.5 h using a Savant speedvac desiccator. The lipid was then allowed to hydrate in distilled H_2O on ice overnight. The hydrated lipid films were sonicated in a bath-type sonicator (Laboratory Supplies, Hicksville, NY) for 10 min, followed by a 10 min resting period, and an additional 10 min of sonication. Hepes buffer, pH 7.5, was then added (20 mM Hepes, 150 mM NaCl final concentration) while vortexing. Cationic liposome/oligonucleotide complexes were prepared by adding oligonucleotide, in Hepes buffer, pH 7.5, to liposomes (final charge ratio 4:1, mol DC-Chol/mol nucleotide) while vortexing. Diameter measurements of liposomes and liposome/oligonucleotide complexes were done using a Malvern 4700c multiangle light-scattering instrument.

2.3. In vitro cell uptake studies

CHO D$^-$ cells were grown in 24-well plates to ~ 80% confluency and then washed in serum-free medium. DC-Chol/DOPE liposomes (1:1, mol/mol) labeled with ^{3}H-CE, and without or with increasing concentration of DTPA-SA, and without or with complexed oligonucleotide, were added to the cells. Serum was isolated from female CD-1 mice as described [11]. Samples added in serum were preincubated with the serum at 37°C for 5 min. All incubations were done at 37°C for 1 h. Cells were then washed three times with serum-free medium and dissolved

overnight in 0.1 M NaOH. An aliquot from each well was assayed for radioactivity by scintillation counting, and the protein content of each well was determined by BCA assay (Pierce, Rockford, IL). Data are expressed as nmol lipid uptake per mg cellular protein. All determinations were done in triplicate.

2.4. Liposome-cell fusion

Lipid mixing between cationic liposomes and cells was assayed as described [12]. Briefly, 80 nmol DC-Chol/DOPE liposomes (1:1, mol/mol) labeled with 5 mol% Pyr-PC were added to 3 ml PBS equilibrated at 37°C. Trypsinized CHO cells ($1 \cdot 10^5$ cells) were then added, and decreasing pyrene excimer fluorescence (λ_{ex} 343 nm and λ_{em} 483 nm, 3 nm slit widths) monitored for 30 min. At the end of the incubation period, Triton X-100 was added to a final concentration of 1.0% and excimer fluorescence F_{Tx} recorded. The extent of lipid mixing was calculated using the equation: % maximal lipid mixing = $100 \times (F_o - F)/(F_o - F_{Tx})$ where F_o and F are the excimer fluorescence intensities before and after the addition of cells, respectively.

2.5. Fluorescence microscopy

CHO D^- cells were grown on 18 mm round glass coverslips to 70–80% confluency. After washing the cells with serum-free RPMI 1640 medium, samples were added and incubated with the cells at 37°C for 1 h. The cells were then washed again with serum-free medium, and fixed in 1% paraformaldehyde for 20 min at room temperature. After a final washing with serum-free medium, the coverslips were mounted onto glass microslides and the cells were observed using a Nikon Microphot FX fluorescence microscope and a 60 × oil immersion lens.

2.6. Iodination of oligonucleotide

Oligonucleotide was iodinated as described [13] with modification. Briefly, 600 pmol ^{125}I was added to 100 μg of oligonucleotide LS2-1 in 0.1 mM sodium acetate, pH 4.0 in a glass tube coated on the bottom with 30 μg Iodogen reagent (Pierce, Rockford, IL). The mixture was incubated in a water bath at 50°C for 30 min. Oligonucleotide was partially reisolated using a Bio-Gel P-4 spin column (Bio-Rad, Richmond, CA). Residual unincorporated iodine was removed by dialysis against distilled water at 4°C overnight using a CE MWCO 500 dialysis membrane (Spectrum, Houston, TX). Purity of the final sample was determined by thin layer chromatography on PEI-cellulose plates (EM Science, Gibbstown, NJ) chromatographed in 0.55 M ammonium sulfate. Analysis of the plates using a Molecular Dynamics PhosphorImager (Sunnyvale, CA) revealed > 95% radioactivity remained at the origin with the oligonucleotide.

2.7. Biodistribution studies

^{111}In-DTPA-SA-labeled liposomes, without or with complexed ^{125}I-labeled oligonucleotide, were injected (0.500 mg of lipid, unless indicated otherwise, in 200 μl) into female CD-1 mice (6–8-week-old) via the tail vein. At the indicated time interval, the mice were anesthetized, weighed, and bled by retroorbital puncture. The mice were killed by cervical dislocation and dissected. In addition to blood, organs were collected, weighed, and analyzed for ^{111}In radioactivity in a gamma counter. For dual-label studies, channel windows were set to collect ^{111}In and ^{125}I cpm individually, and cross-talk was accounted for appropriately. The results are presented as percent of the total injected dose for each organ. The total radioactivity in blood was determined by assuming the total blood volume was 7.3% of the body weight [14]. Blood correction factors for each organ were determined as described [15] for female CD-1 mice of the same age and weight. Approx. 4, 8, and 1% of the total blood remained in the lung, liver, and spleen, respectively, following bleeding.

2.8. Immuno-histochemistry

For immuno-histochemistry and immuno-electron microscopy, tissues from mice injected with cationic liposome/oligonucleotide F15-27 complex (830 μg of lipid in 400 μl) i.v. via the tail vein were collected at 15 min and 24 h post-injection. The mice were killed by cervical dislocation and the lungs were inflated in situ with 4% paraformaldehyde in 0.1 M phosphate buffer (PB), pH 7.4, then excised and immersed in the fixative. The livers were removed whole, then thinly sliced, and immersion fixed. Small blocks of the lung and liver were further processed for immuno-electron microscopy (see below). The remaining lung and liver samples were rinsed overnight in PB buffer and then processed into paraffin. Tissue sections cut at 3 μm were deparaffinized and hydrated into PBS, then pretreated with 0.1% proteinase for 1 min and with 2 N HCl for 1 h at room temperature. After thorough washing with distilled water, sections were incubated with rat monoclonal antibody F4/80 (Harlan, Indianapolis, IN), an antibody which binds to mouse macrophage [16], or isotype control at a concentration of 200 μg/ml. Primary antibody was detected by using ABC reagents from BioTek for peroxidase immuno-histochemistry with diaminobenzidine as brown chromagen. Sections were then incubated with rat anti-BrdU antibody (Accurate, Westbury, NY) or isotype control at a concentration of 1 μg/ml for 45 min. This antibody was subsequently detected using the ABC-alkaline phosphatase reagents and red chromagen from BioTek (Santa Barbara, CA). Sections were counterstained with hematoxylin, dehydrated, cleared, and coverslipped.

2.9. Immuno-electron microscopy

For immuno-electron microscopy, lung and liver blocks were fixed for 3 h. These specimens were subsequently

washed overnight in PB and dehydrated through a graded ethanol series and propylene oxide prior to infiltration in Medcast resin (Ted Pella, Redding, CA) and curing at 60°C for 24 h. Ultrathin sections were cut and collected on nickel grids. The section faces were hydrated in PBS for 30 min and incubated for 2 h with either rat anti-BrdU primary antibody (Dako, Carpenteria, CA) or an isotype control at a concentration of 33 μg/ml in a diluent consisting of 1% bovine serum albumin in PBS with 0.05% Tween and 0.02% NaN_3. After washing three times in PBS, the tissues were blocked by incubating in 10% goat serum in diluent for 1 h. The sections were then directly reacted for 1 h with a 5% solution of 10 nm gold-goat anti-rat (GAR) secondary antibody conjugate (Amersham, Buckinghamshire, UK) in diluent. The sections were rinsed in PBS, then in distilled water and subsequently contrast enhanced with aqueous uranyl acetate prior to examination on a Phillips CM120 transmission electron microscope.

3. Results

3.1. Analysis of DTPA-SA in cationic liposomes

DTPA-SA has been used extensively to monitor liposome biodistribution [10,11,15,17]. Before conducting cationic liposome biodistribution studies, DTPA-SA was examined for any influence on various properties of cationic liposomes. Increasing mol% of DTPA-SA was included in cationic liposomes (DC-Chol/DOPE, 1:1, mol/mol, and labeled with a trace amount of ^{3}H-CE) to determine if this molecule influences liposome uptake by CHO cells. Fig. 1A shows that inclusion of up to 5 mol% DTPA-SA in the lipid composition did not affect uptake. Furthermore, liposome formation and liposome size were not influenced by the added DTPA-SA (data not shown). Fusion of the cationic liposomes with endosomal/lysosomal membranes following uptake may play an important role in oligonucleotide delivery [12]. Inclusion of up to 5 mol% DTPA-SA in cationic liposomes labeled with Pyr-PC did not significantly influence lipid mixing following uptake by CHO cells, as monitored by decreasing excimer fluorescence (Fig. 1B). Finally, inclusion of up to 5 mol% DTPA-SA in cationic liposomes did not influence nuclear delivery of FITC-labeled oligonucleotide to CHO cells (Fig. 1C–E). Therefore, because DTPA-SA did not affect cationic liposome formation, interaction with cells, or oligonucleotide delivery, this amphipathic chelator was used as a lipid phase radiolabel for further investigations, where the concentration of DTPA-SA (labeled with a trace of ^{111}In) never exceeded 0.2 mol%.

3.2. Biodistribution of cationic liposomes

Cationic liposomes with increasing positive charge (20–80 mol% DC-Chol) were prepared and their biodistributions determined at 24 h post i.v. injection. No significant differences in biodistribution amongst the liposome compositions were observed (Table 1). The injected liposomes accumulated primarily in liver (~ 74–82% of the injected dose). Accumulation in spleen (~ 4–8% of the injected dose) and skin (~ 3–5% of the injected dose) was also observed. Approx. 1% or less of the injected dose accumulated in lung. Thus, the majority of the injected lipid accumulated in liver.

The uptake of injected cationic liposomes (DC-Chol/DOPE, 1:1, mol/mol) by liver was very rapid as shown in Fig. 2A. By 5 min post-injection, approx. 60% of the injected dose had accumulated in liver, while only approx. 18% of the injected dose remained in circulation. By 7.5 h post-injection liver uptake was saturated, where accumulation of approx. 85% of the injected dose was achieved.

3.3. Effect of injection dose on cationic liposome biodistribution

The injection dose of cationic liposomes (DC-Chol/DOPE, 1:1, mol/mol) was varied from 0.083 mg to 1.670 mg of lipid in 200 μl, and the mice were killed at 24 h post-injection. The results are presented in Fig. 3 as μg of lipid accumulated per g of tissue, plotted against mg of lipid injected per kg weight of the mice. Liposome uptake in spleen and liver was directly proportional to the injected dose in the range of 0.083 to 0.833 mg per mouse, or 3.33 to 33.33 mg/kg body weight. Within this range, spleen and liver accumulation were equally efficient. However, at an injection dose of 66.80 mg/kg body weight, the efficiency of the spleen uptake increased relative to that of liver uptake. Furthermore, the concentration of lipid in lung and blood slightly increased at the high doses. This effect may have resulted from saturation of the liver uptake mechanism(s) at the high dose, allowing opportunity for the liposomes to circulate longer and accumulate in other tissues.

3.4. Effect of serum on cationic liposome uptake in vitro

Interaction of cationic liposomes with plasma components immediately following injection may hinder nonspecific binding with cell membranes and accumulation within tissues. This would explain for example the relatively low accumulation of cationic liposomes in lung, the first capillary bed encountered following tail vein injection. To explore the effects of plasma components, cationic liposomes were briefly preincubated in increasing concentrations of mouse serum, and the mixtures were subsequently added to CHO cells for 1 h incubation at 37°C. Fig. 4A shows that increasing concentration of serum blocked cationic liposome binding/uptake by CHO cells. The presence of only 10% serum reduced uptake by 80% compared to serum-free incubations. Thus, components in the plasma

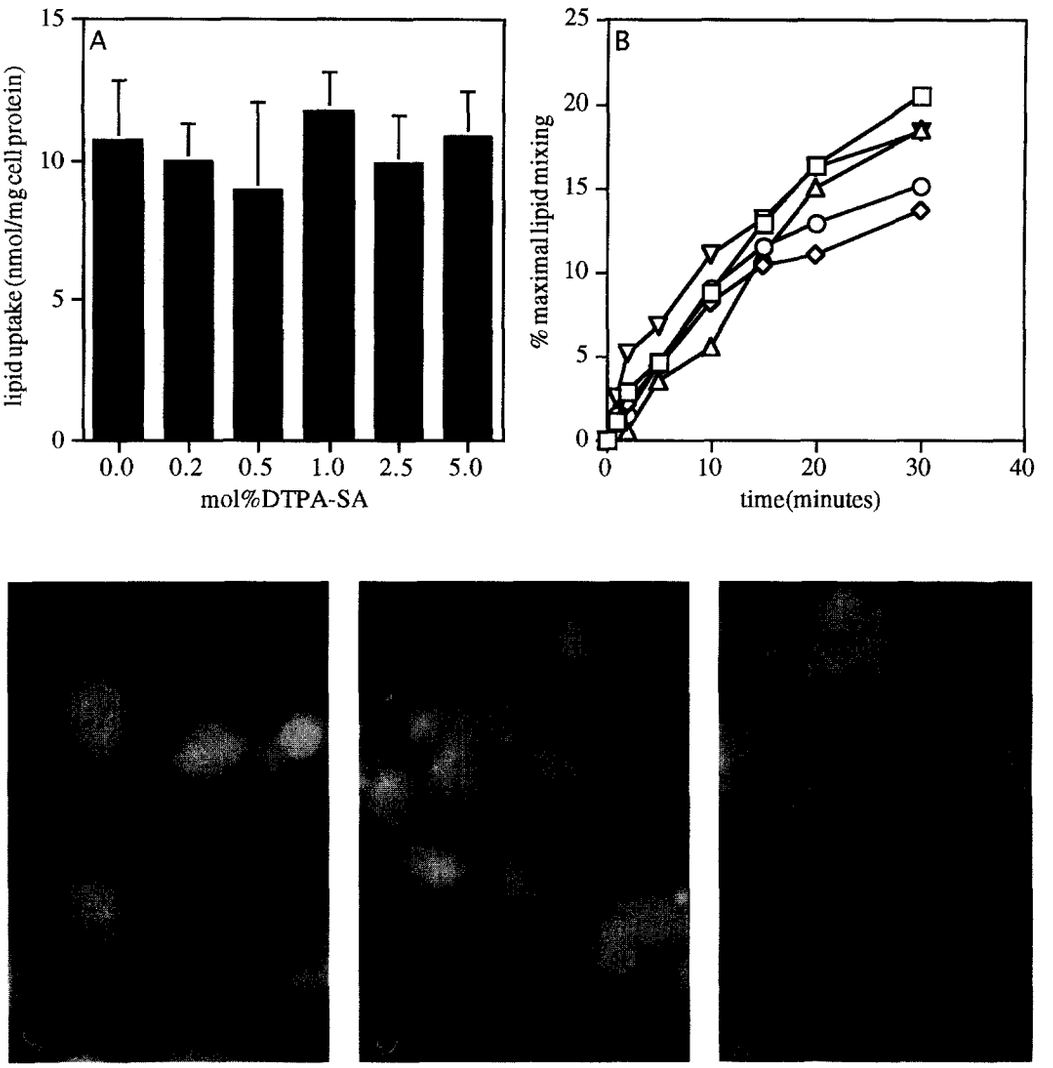

Fig. 1. DTPA-SA does not affect properties of cationic liposomes. (A) Binding/uptake of cationic liposomes by CHO cells is unaffected by DTPA-SA. DC-Chol/DOPE liposomes with increasing concentration of DTPA-SA, and labeled with ^{3}H-CE, were incubated with CHO cells for 1 h at 37°C. The liposome concentration in each sample was 80 μM. The cells were then washed, lysed, and radioactivity and protein concentration assayed as described in Materials and methods. The data represent the mean ± S.D. for samples assayed in triplicate. (B) Fusion of cationic liposomes with CHO cells is unaffected by DTPA-SA. Lipid mixing between DC-Chol/DOPE liposomes, with 5 mol% Pyr-PC and 0.0 (□), 0.2 (◇), 1.0 (○), 2.5 (△), and 5.0 (▽) mol% DTPA-SA, and trypsinized CHO cells at 37°C was assayed as described in Section 2. (C–E) Delivery of oligonucleotide to cells by cationic liposomes is unaffected by DTPA-SA. DC-Chol/DOPE liposomes with 0.0 (C), 2.5 (D), and 5.0 (E) mol% DTPA-SA, and complexed with FITC-labeled oligonucleotide, were incubated with CHO cells grown on coverslips for 1 h at 37°C. The liposome concentration in each sample was 100 μM. The cells were then washed, fixed, and photographed as described in Section 2.

may indeed hinder nonspecific binding of cationic liposomes to cells.

3.5. Biodistribution of cationic liposome / oligonucleotide complex

Dual-radiolabeled cationic liposome/oligonucleotide complex was prepared by adding oligonucleotide, labeled with a trace of ^{125}I-oligonucleotide, to ^{111}In-DTPA-SA-labeled cationic liposomes. The size of the complex was approx. 1828 ± 24 nm (polydispersity = 0.36) as measured by light-scattering, compared to a measured size of 65 ± 1 nm (polydispersity = 0.25) for the liposomes before addition of oligonucleotide (data not shown). The biodistribution of the complex injected i.v., following the lipid label, and compared to that of liposomes without added oligonucleotide, is shown in Fig. 2B. Complexation with oligonucleotide induced a dramatic and transient accumulation of lipid in lung. At 5 min post-injection, ~ 80% of the injected dose of the complexed lipid was present in lung compared to ~ 10% of the injected dose for liposomes without added oligonucleotide. This accumulated lipid gradually redistributed to liver where by 18 h post-injection, approx. 4% and 82% of the injected dose of lipid were present in lung and liver, respectively.

The biodistribution of the complex following the oligo-

Table 1
Biodistribution of cationic liposomes at 24 h post-injection [a]

Tissue	% Injected dose				
DOPE/DC-Chol (mol/mol):	4:1	2:1	1:1	1:2	1:4
Blood [b]	0.38 (0.07)	0.35 (0.11)	0.40 (0.04)	0.41 (0.12)	0.35 (0.06)
Heart	0.08 (0.01)	0.06 (0.02)	0.08 (0.01)	0.08 (0.02)	0.08 (0.01)
Thymus	0.04 (0.01)	0.04 (0.03)	0.03 (0.03)	0.04 (0.03)	0.02 (0.03)
Lung	0.48 (0.09)	0.65 (0.13)	0.92 (0.21)	0.76 (0.11)	1.13 (0.15)
Liver	74.17 (5.80)	77.43 (1.46)	82.18 (1.11)	75.89 (6.68)	77.65 (0.64)
Kidney	0.75 (0.11)	0.68 (.10)	0.82 (0.15)	0.67 (0.13)	0.68 (0.06)
Spleen	7.77 (2.04)	6.35 (1.69)	4.55 (0.84)	3.92 (0.73)	4.67 (1.28)
Stomach	0.70 (0.96)	0.25 (0.13)	0.21 (0.02)	1.43 (2.21)	0.12 (0.03)
Intestine	1.40 (0.36)	1.72 (0.11)	2.12 (0.52)	2.30 (0.15)	1.89 (0.40)
Pancreas	0.04 (0.01)	0.09 (0.10)	0.08 (0.05)	0.15 (0.15)	0.10 (0.06)
Lymph nodes [c]	0.00 (0.01)	0.00 (0.01)	0.01 (0.02)	0.04 (0.03)	0.01 (0.01)
Bone marrow	n.d. [d]	n.d.	n.d.	n.d.	n.d.
Uterus	0.06 (0.02)	0.07 (0.04)	0.08 (0.02)	0.14 (0.07)	0.18 (0.05)
Ovaries	0.03 (0.01)	0.03 (0.01)	0.03 (0.01)	0.09 (0.05)	0.07 (0.06)
Skeletal muscle [e]	0.80 (0.20)	0.99 (0.35)	0.74 (0.24)	0.92 (0.13)	1.14 (0.43)
Skin [f]	3.29 (0.66)	4.54 (2.67)	3.13 (0.15)	3.39 (0.30)	4.33 (0.71)
Brain	0.01 (0.02)	0.02 (0.01)	0.02 (0.02)	0.01 (0.01)	0.07 (0.04)
Tail (injection site)	0.43 (0.16)	0.46 (0.11)	0.43 (0.11)	0.50 (0.11)	0.51 (0.19)
% recovery [g]	90.42 (2.52)	93.74 (3.51)	95.84 (0.97)	90.73 (3.29)	92.99 (1.56)

[a] Cationic liposomes prepared by sonication, with increasing concentration of DC-Chol, and labeled with ^{111}In-DTPA-SA were injected i.v. (500 μg of lipid in 200 μl) into CD-1 mice. Percent injected dose was measured 24 h post-injection. Numbers in parentheses are S.D. ($n = 3$).
[b] Calculated from collected blood and assuming that 7.3% of the total body weight is blood [14].
[c] Only mesenteric lymph nodes were collected.
[d] Not detected.
[e] Calculated from collected muscle from the hind legs and assuming that 50% of the total body weight is muscle [18].
[f] Calculated from skin collected from the abdomen and neck, and assuming that 11% of the total body weight is skin [18].
[g] (Sum of cpm from collected tissues divided by injected cpm) × 100.

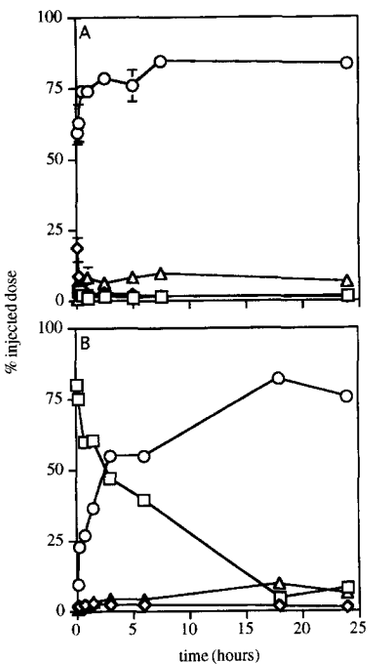

Fig. 2. Time-course for biodistribution of cationic liposomes and cationic liposome/oligonucleotide complex. DC-Chol/DOPE liposomes labeled with ^{111}In-DTPA-SA and without (A) or with (B) complexed oligonucleotide (cationic lipid/nucleotide charge ratio = 4:1) were injected i.v. (0.500 mg of lipid in 200 μl). Percent injected dose in blood (◇), liver (○), spleen (△), and lung (□) was measured at the indicated time intervals. Bars represent S.D. ($n = 3$).

nucleotide label was similar to the results obtained following the lipid label. Again, an immediate yet transient accumulation in lung was observed (Fig. 5A). However, the recovery of radioactivity was comparatively less than that from the lipid label and may be attributed to instability of the iodine label. The accumulation of the oligonucleotide in liver appears to plateau at 3 h post-injection. This

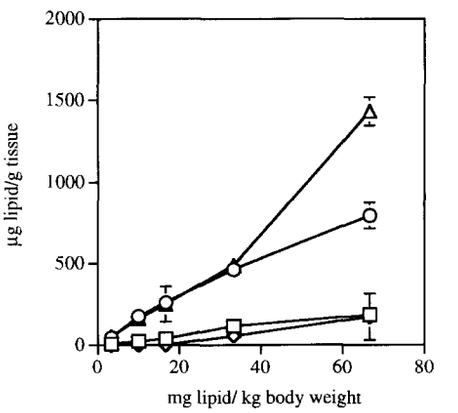

Fig. 3. Effect of injection dose on cationic liposome biodistribution. Various doses of DC-Chol/DOPE liposomes labeled with ^{111}In-DTPA-SA were injected i.v. in a volume of 200 μl and the percent injected dose in blood (◇), liver (○), spleen (△), and lung (□) measured at 24 h post-injection. Bars represent S.D. ($n = 3$). The results are expressed as μg of lipid accumulated per g of tissue weight.

apparent plateau however may reflect metabolism of the labeled oligonucleotide. Indeed, a transient increase of label present in intestine peaked at 3 h post-injection, followed by an increased appearance of label in feces (Fig. 5B). Excretion of label in urine was also observed. Therefore, the liver accumulation of the liposome/oligonucleotide complex likely increased beyond 3 h post-injection, as revealed following the relatively nonmetabolizable lipid label [17].

We speculate that following injection, the complex accumulates rapidly in lung due to embolism. For oligonucleotide injected without complexed lipid, approx. 0.7% of the injected dose accumulated in lung at 15 min post-injection (data not shown), suggesting that the oligonucleotide did not actively target the complex to lung. We further speculate that interaction with plasma components inhibits cellular uptake of the complex in lung. The complex is then slowly released from lung, perhaps caused by the flow of blood, and is immediately removed from the circulation by the liver. This immediate removal, perhaps mediated by bound opsonin(s), is indicated by lack of appearance of lipid in the blood, and the inverse pharmacokinetic relation of lung and liver accumulation (Fig. 2B).

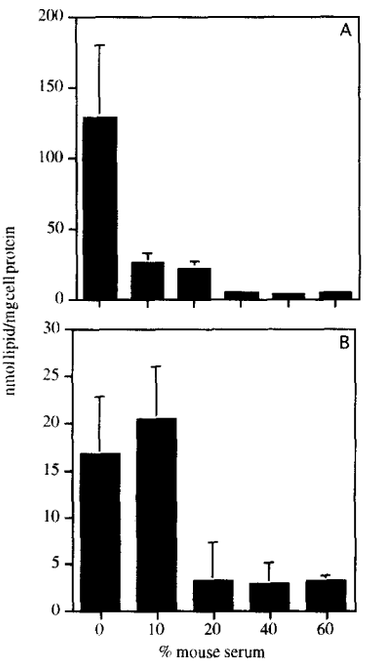

Fig. 4. Effect of serum on binding/uptake of cationic liposomes and cationic liposome/oligonucleotide complex by CHO cells. CHO cells were incubated with ^{3}H-CE-labeled DC-Chol/DOPE liposomes, without (A) or with (B) complexed oligonucleotide (cationic lipid/nucleotide charge ratio = 4:1), in the presence of increasing concentration of mouse serum for 1 h at 37°C. The concentration of liposomes added to each well was 80 μM. The cells were then washed, and cpm and protein concentration in each well determined. The data represent the mean ± S.D. for samples assayed in triplicate.

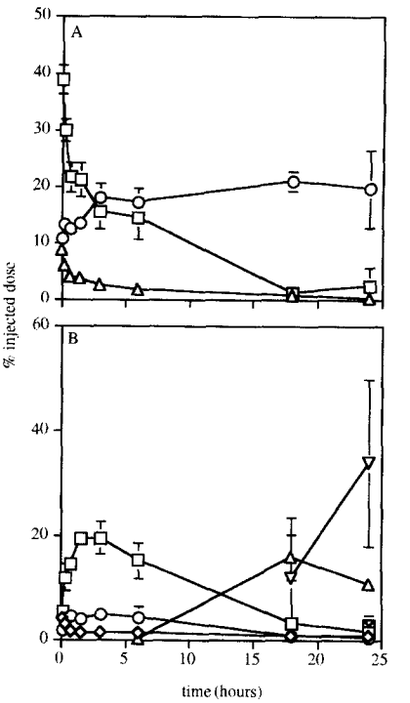

Fig. 5. Biodistribution of oligonucleotide complexed with cationic liposomes. Liposomes complexed with oligonucleotide (cationic lipid/nucleotide charge ratio = 4:1, oligonucleotide labeled with a trace amount of ^{125}I-oligonucleotide) were injected i.v. (0.500 mg of lipid and 0.031 mg oligonucleotide in 200 μl). Percent injected dose in (A) lung (□), liver (○), and blood (△), and (B) kidney (◇), stomach (○), intestine (□), feces (△), urine (▽), and thyroid (⊠, 24 h only) was measured at the indicated time intervals. Bars represent S.D. ($n = 3$).

3.6. Effect of serum on cationic liposome / oligonucleotide complex uptake in vitro

To test the hypothesis that plasma components inhibit cellular uptake of the cationic liposome/oligonucleotide complex, the complex was briefly preincubated with increasing concentration of mouse serum, and the mixtures were subsequently added to CHO cells for 1 h incubation at 37°C. The presence of only 20% mouse serum was sufficient to reduce binding/uptake of the complex by 81% compared to serum-free incubations (Fig. 4B). A higher concentration of serum however was required to inhibit binding/uptake of the complex compared to cationic liposomes without added oligonucleotide (Fig. 4A). These results nonetheless support the hypothesis that plasma components inhibit cellular uptake of the complex.

3.7. Tissue distribution of cationic liposome / oligonucleotide complex

The distribution of the cationic liposome/oligonucleotide complex within lung and liver at 15 min and 24 h post i.v. injection is shown in Fig. 6. BrdU-labeled oligonucleotide in the tissue sections was stained using anti-BrdU antibody and alkaline phosphatase-conjugated secondary

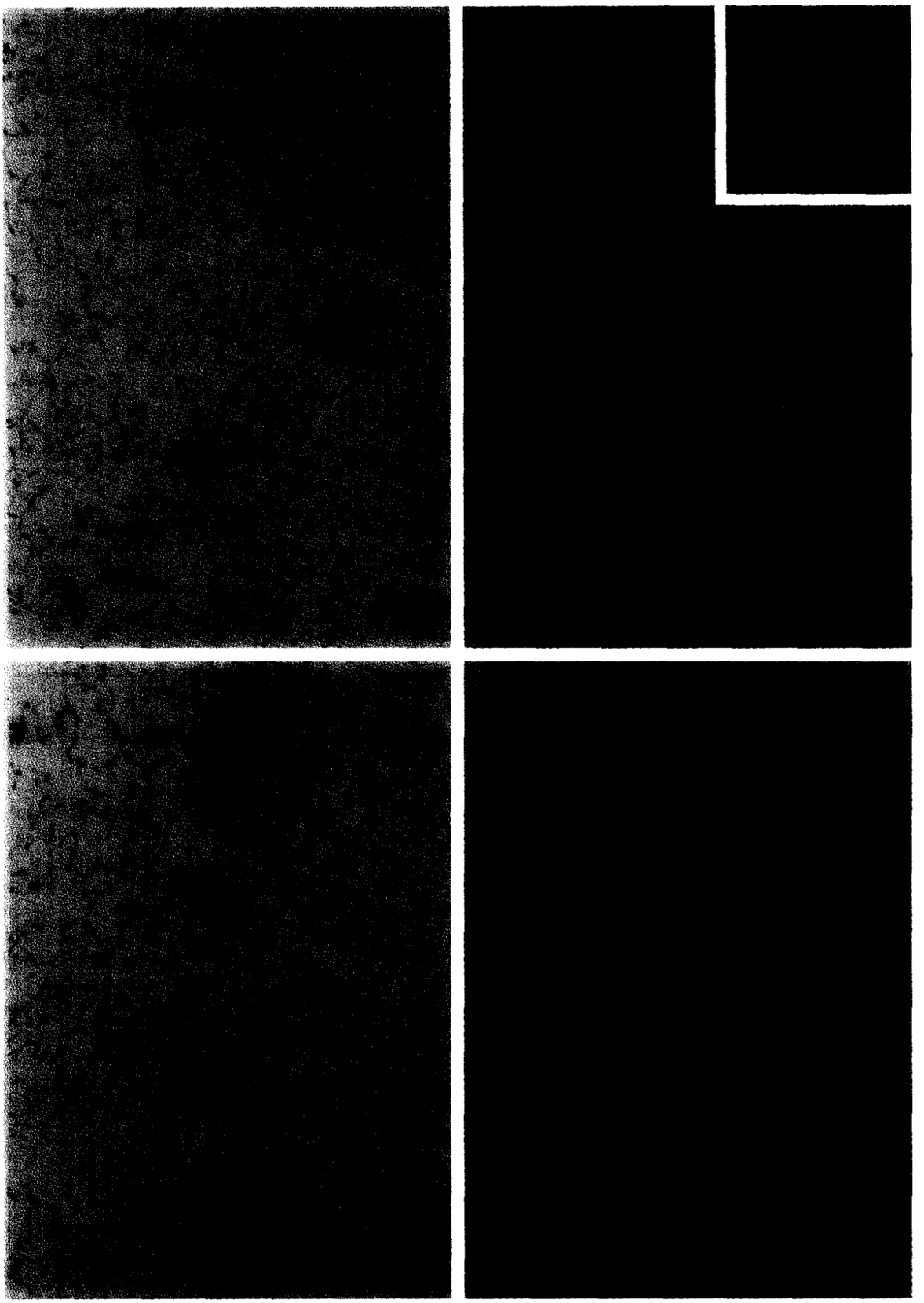

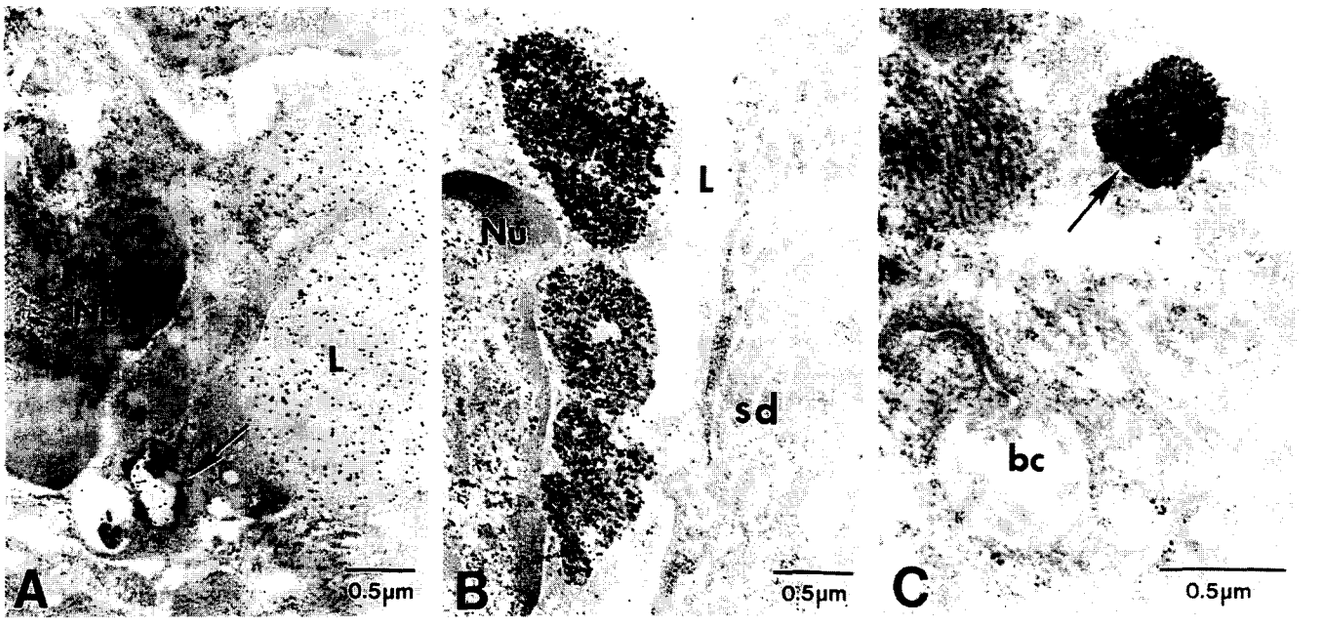

Fig. 7. Localization of liposome/oligonucleotide complex accumulated in tissues as determined by immuno-electron microscopy. Mice were injected with cationic liposome/oligonucleotide F15-27 complex (cationic lipid/nucleotide charge ratio = 4:1, 830 μg of lipid in 400 μl injected) i.v. via the tail vein. Tissues were harvested and processed as described in Section 2. The BrdU-labeled oligonucleotide was stained with rat anti-BrdU antibody and gold-GAR secondary antibody conjugate. The sections were contrast enhanced with aqueous uranyl acetate. (A) Lung section from mouse killed at 15 min post-injection. (B and C) Liver section from mouse killed at 24 h post-injection. Arrow in (A) indicates uptake of oligonucleotide into vacuoles of macrophage. Arrow in (C) indicates presence of oligonucleotide in lysosome of hepatocyte. Nu, nucleus; L, lumen; sd, space of Disse; and bc, bile canaliculis. Bars in (A–C) correspond to 0.5 μm.

antibody with red chromagen. Fig. 6A reveals large aggregates of oligonucleotide within the alveolar septa at 15 min post-injection. By 24 h post-injection, the degree of staining within lung sections decreased, with fewer aggregates and which were of smaller size remaining (Fig. 6B). These results support embolism as the mechanism by which the injected complex accumulates rapidly in lung following injection. Furthermore, the staining intensities of the lung and liver sections (see below) correspond to the quantitative results obtained from the radiolabel studies. Staining of macrophage in the lung sections with the brown chromagen is difficult to discern at the magnification shown.

Fig. 6C shows the distribution of Kupffer cells, stained with brown chromagen, within the liver section from a mouse sacrificed at 15 min post-injection. Discernible staining of the oligonucleotide was difficult to detect at this early time point. By 24 h post-injection, liver accumulated oligonucleotide was localized primarily to Kupffer cells, where co-localization of stains was observed (Fig. 6D). Higher magnification revealed oligonucleotide accumulated within Kupffer cells to be present in the cytoplasm (Fig. 6D, inset), and not in the nucleus. A detectable amount of oligonucleotide however was present in non-macrophage cells (Fig. 6D).

Distribution of the injected cationic liposome/oligonucleotide complex within lung and liver was further evaluated by immuno-electron microscopy (Fig. 7). BrdU-labeled oligonucleotide in tissue sections was stained with rat anti-BrdU antibody and gold-GAR secondary antibody conjugate. At 15 min post-injection, oligonucleotide accumulated in lung was localized primarily to the lumen of pulmonary capillaries (Fig. 7A). Oligonucleotide was also occasionally present within phagocytic vacuoles of macrophage in the lung (Fig. 7A). These results give further support for embolism as a mechanism for early lung accumulation of the injected complex.

In liver, oligonucleotide was abundantly present in phagocytic vacuoles of Kupffer cells at 24 h post-injection

Fig. 6. Localization of liposome/oligonucleotide complex accumulated in tissues as determined by immuno-histochemistry. Mice were injected with cationic liposome/oligonucleotide F15-27 complex (cationic lipid/nucleotide charge ratio = 4:1, 830 μg of lipid in 400 μl injected) i.v. via the tail vein. Tissues were harvested and processed as described in Section 2. The BrdU-labeled oligonucleotide was stained with anti-BrdU antibody and alkaline phosphatase-conjugated secondary antibody with red chromagen. Macrophage in tissue sections were stained with monoclonal antibody F4/80 and peroxidase-conjugated secondary antibody with diaminobenzidine as a brown chromagen. Tissue sections were counterstained with hematoxylin. (A and B) Lung sections from mice sacrificed at 15 min (A) and 24 h (B) post-injection. Bar in (A) corresponds to 100 μm for lung sections. (C and D) Liver sections from mice killed at 15 min (C) and 24 h (D) post-injection. Bar in (C) corresponds to 50 μm for liver sections. Arrow and arrowhead in (D) indicate presence of oligonucleotide in a Kupffer cell and a nonmacrophage cell, respectively. (D, inset) Liver section prepared as in (D) viewed at high magnification. Arrow in (D, inset) indicates presence of oligonucleotide within Kupffer cells.

(Fig. 7B). Oligonucleotide was also infrequently found within lysosomes of hepatocytes (Fig. 7C). Immuno-electron microscopy did not reveal any notable presence of oligonucleotide in nuclei of lung or liver cells. Furthermore, presence of oligonucleotide within endothelial cells of these tissues was not detected.

4. Discussion

We have used DTPA-SA as a lipophilic radiolabel to evaluate the biodistribution of cationic liposomes in mice following intravenous injection. This amphipathic chelating agent consists of DTPA covalently attached to two stearyl chains via amide bonds [19]. It has previously been demonstrated that this radiolabel is not transferred to serum components from liposomes [19], and is not rapidly metabolized in vivo [17]. The negative charge contributed by this amphipathic chelator, with three carboxylic acid groups per molecule, might be expected to interfere with the formation and activity of cationic liposomes. However, we have shown here that this label, at concentrations of up to 5 mol%, does not interfere with properties of cationic liposomes, including oligonucleotide delivery.

The clearance of positively charged SUVs containing stearylamine (SA) has previously been shown to be similar to that of neutral liposomes, and less rapid than negatively charged liposomes with phosphatidylserine (PS) in the lipid composition [20]. However, issues concerning removal of the positively charged SA component following injection, thus leading to uncharged vesicles were presented [21]. Clearance of liposomes which retain their positively charged lipid component may be through interaction with the negative surface charge of cells and/or interaction with negatively charged plasma components, including opsonin(s). We have demonstrated here that the presence of serum blocks the binding/uptake of DC-Chol-containing vesicles by cells in vitro. Furthermore, the liposomes did not accumulate significantly in lung, suggesting binding/uptake by endothelial cells of the lung was inhibited by plasma components. It has been shown that positively charged liposomes assume an overall negative charge in the presence of plasma [22], which may be contributed by bound negatively charged plasma protein. We therefore speculate that clearance of DC-Chol vesicles, by the reticuloendothelial system, is primarily mediated via rapidly bound protein, including opsonin(s). To determine whether there is any significant transfer of DC-Chol from the vesicles to serum components, however, requires further investigation.

The cationic liposome/oligonucleotide complex demonstrated a dramatic, yet transient accumulation in lung after injection, as revealed following both radiolabeled lipid and oligonucleotide. Because the lipid label is not rapidly metabolizable [17], these data indicate the loss of accumulated radioactivity from the lung is not due to secretion of endocytosed and metabolized label. We speculate that the complex was not readily endocytosed by lung cells, except for a small portion by lung macrophage, and was accumulated by embolism. We have shown that serum blocks binding/uptake of the cationic liposome/oligonucleotide complex by CHO cells in vitro. The molar charge ratio of DC-Chol to nucleotide in the present studies was 4:1, allowing for residual positive charge for efficient oligonucleotide delivery (D. Collins, unpublished data). Electrostatic attraction of negatively charged plasma components to the complex may have in turn inhibited interaction of the complex with cells. Interestingly, a greater concentration of serum was required to inhibit binding/uptake of the complex compared to cationic liposomes without oligonucleotide. One possible explanation is that while a reduction in positive charge upon complexation with oligonucleotide reduced lipid uptake in the absence of serum, the complexation furthermore reduced the electrostatic attraction of serum components. Size measurements of the complex, before injection, by light-scattering routinely revealed average diameters of approx. 2 μm. Furthermore, the size and stability of the complex may be modified following injection. A sufficiently large size/aggregation of the complex would allow for physical trapping in the pulmonary capillaries as emboli. The degree to which serum-complex interaction may contribute to the actual aggregation/embolization requires further characterization. While bound serum components may have inhibited cellular uptake of the complex, these components may have included opsonin(s) to mediate the rapid clearance, primarily by Kupffer cells of the liver, following release from the lung.

As demonstrated here, a small portion of oligonucleotide accumulated in liver at 24 h was detected in the lysosomes of hepatocytes. To determine why these cells endocytosed oligonucleotide yet did not reveal detectable nuclear delivery requires further investigation. Overall, it must be noted that by our immuno-histochemistry and immuno-electron microscopy methods, nuclear delivery of oligonucleotide by cationic liposomes in vivo was not detected. This includes nuclear delivery to hepatocytes and macrophages of the liver and macrophages of the lung which accumulated oligonucleotide, as well as for endothelial cells where even uptake of oligonucleotide was not observed. In other studies, our methods have successfully demonstrated accumulation of oligonucleotide in the nuclei of smooth muscle cells when administered to injured arteries [23].

From these studies we propose that interaction with plasma components presents a major hurdle for efficient oligonucleotide delivery by cationic liposomes in vivo. This interaction may inhibit cellular binding/uptake and furthermore mediate rapid clearance by Kupffer cells. By reducing the interaction of plasma components with the injected complex, these barriers to oligonucleotide delivery via cationic liposomes may be overcome.

References

[1] Akhtar, S. and Juliano, R.L. (1992) Trends Cell Biol. 2, 139–144.
[2] Fisher, T.L., Terhorst, T., Cao, X. and Wagner, R. W. (1993) Nucleic Acids Res. 21, 3857–3865.
[3] Agrawal, S., Temsamani, J. and Tang, J.Y. (1991) Proc. Natl. Acad. Sci. USA 88, 7595–7599.
[4] Wagner, R.W. (1994) Nature 372, 333–335.
[5] Bennett, C.F., Chiang, M.Y., Chan, H., Shoemaker, J.E. and Mirabelli, C.K. (1992) Mol. Pharmacol. 41, 1023–1033.
[6] Colige, A., Sokolov, B.P., Nugent, P., Baserga, R. and Prockop, D.J. (1993) Biochemistry 32, 7–11.
[7] Gao, X. and Huang, L. (1991) Biochem. Biophys. Res. Commun. 179, 280–285.
[8] Plautz, G.E., Yang, Z.Y., Wu, B.Y., Gao, X., Huang, L. and Nabel, G.J. (1993) Proc. Natl. Acad. Sci. USA 90, 4645–4649.
[9] Kabalka, G.W., Buonocore, E., Hubner, K., Moss, T., Norley, N. and Huang, L. (1987) Radiology 163, 255–258.
[10] Maruyama, K., Kennel, S.J. and Huang, L. (1990) Proc. Natl. Acad. Sci. USA 87, 5744–5748.
[11] Litzinger, D.C., Buiting, A.M.J., Van Rooijen, N. and Huang, L. (1994) Biochim. Biophys. Acta 1190, 99–107.
[12] Wrobel, I. and Collins, D. (1995) Biochim. Biophys. Acta 1235, 296–304.
[13] Piatyszek, M.A., Jarmolowski, A. and Augustyniak, J. (1988) Anal. Biochem. 172, 356–359.
[14] Wu, M.S., Robbins, J.C., Bugianesi, R.L., Ponpipom, M.M. and Shen, T.Y. (1981) Biochim. Biophys. Acta 674, 255–258.
[15] Litzinger, D.C. and Huang L. (1992) Biochim. Biophys. Acta 1104, 179–187.
[16] Austyn, J.M. and Gordon, S. (1981) Eur. J. Immunol. 11, 805–815.
[17] Holmberg, E., Maruyama, K., Litzinger, D.C., Wright, S., Davis, M., Kabalka, G. W., Kennel, S.J. and Huang, L. (1989) Biochem. Biophys. Res. Commun. 165, 1272–1278.
[18] Burka, L.T., Sanders, J.M., Kool, C.P., Kim, Y.S. and Mathews, H.B. (1987) Toxicol. Appl. Pharmacol. 87, 121–126.
[19] Kabalka, G.W., Davis, M.A., Moss, T.H., Buonocore, E., Hubner, K., Holmberg, E., Maruyama, K. and Huang, L. (1991) Magn. Reson. Med. 19, 406–415.
[20] Juliano, R.L. and Stamp, D. (1975) Biochem. Biophys. Res. Commun. 63, 651–658.
[21] Tan, L. and Gregoriadis, G. (1989) Biochem. Soc. Trans. 17, 690–691.
[22] Black, C. and Gregoriadis, G. (1976) Biochem. Soc. Trans. 4, 253–256.
[23] Farrell, C.L., Bready, J. V., Kaufman, S., Qian, Y. and Burgess, T.L. (1995) Antisense Res. Dev., in press.